Fig. S1

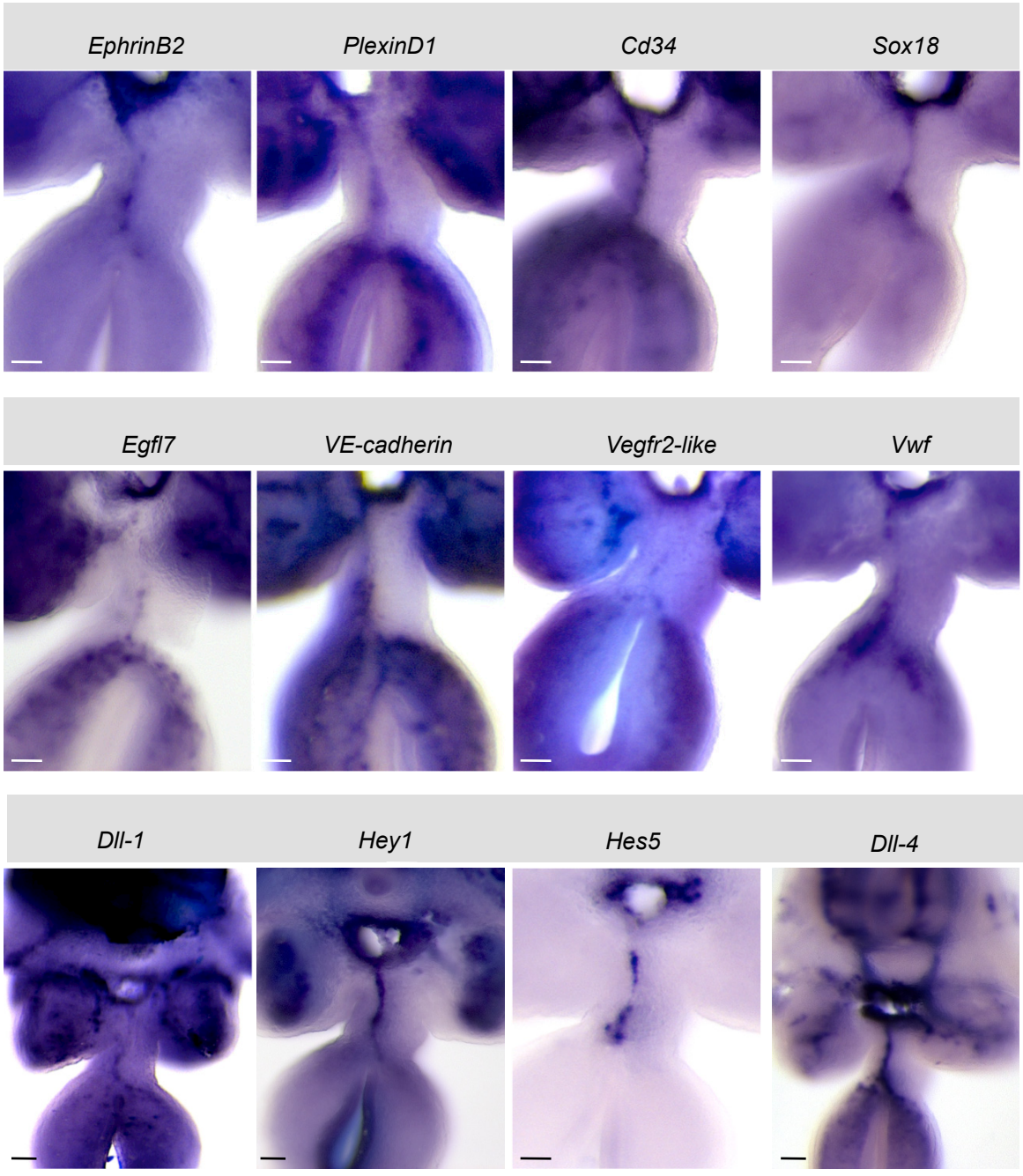
EphrinB2
PlexinD1
Cd34
Sox18
Egfl7
VE-cadherin
Vegfr2-like
Vwf
Dll-1
Hey1
Hes5
Dll-4

Fig. S2

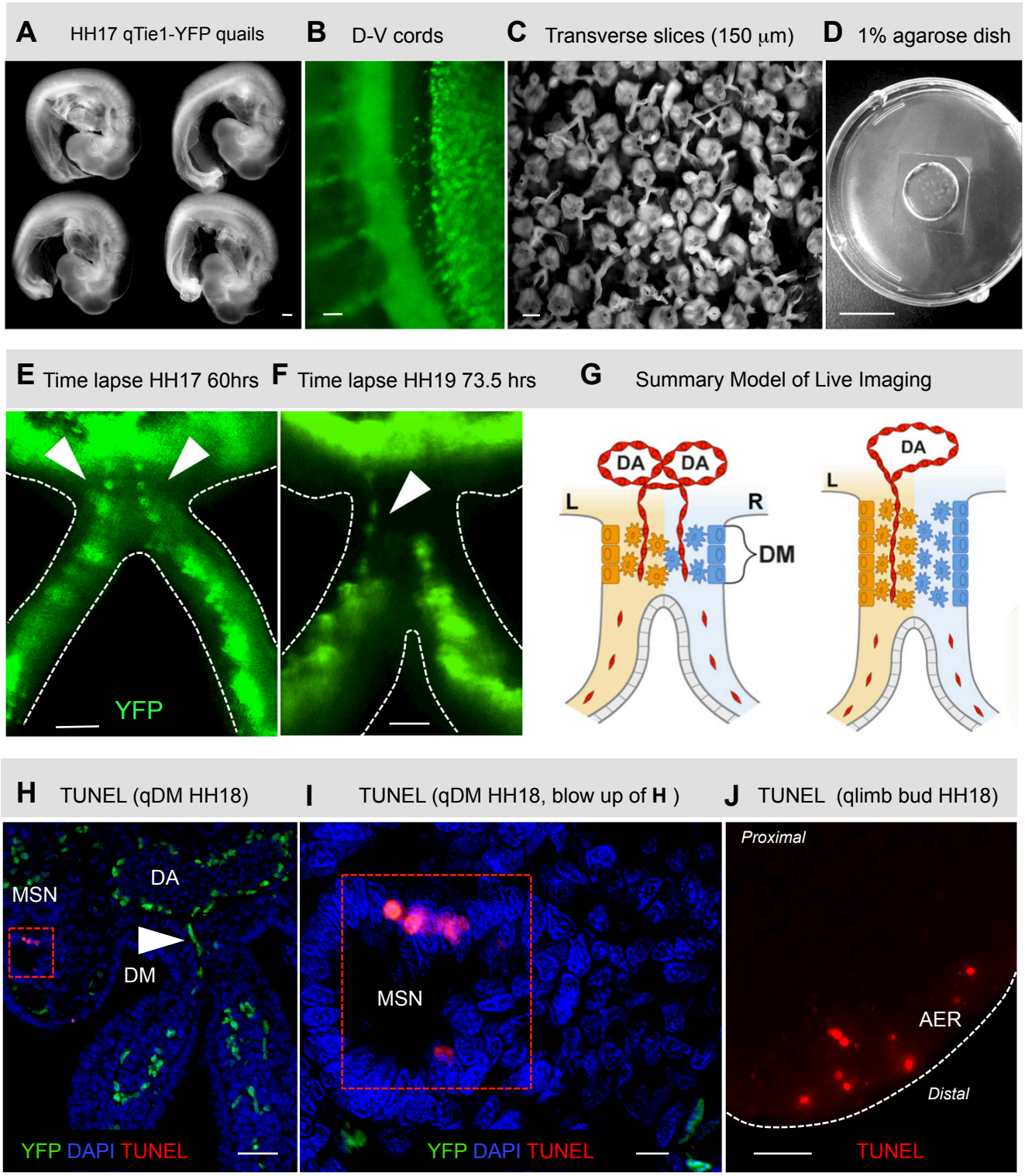
A HH17 qTie1-YFP quails
B D-V cords
C Transverse slices (150 μm)
D 1% agarose dish
E Time lapse HH17 60hrs
F Time lapse HH19 73.5 hrs
G Summary Model of Live Imaging
YFP
DA
DA
L
R
DM
DA
L
H TUNEL (qDM HH18)
I TUNEL (qDM HH18, blow up of H)
J TUNEL (qlimb bud HH18)
MSN
DA
DM
YFP DAPI TUNEL
MSN
YFP DAPI TUNEL
Proximal
AER
Distal
TUNEL

Fig. S3

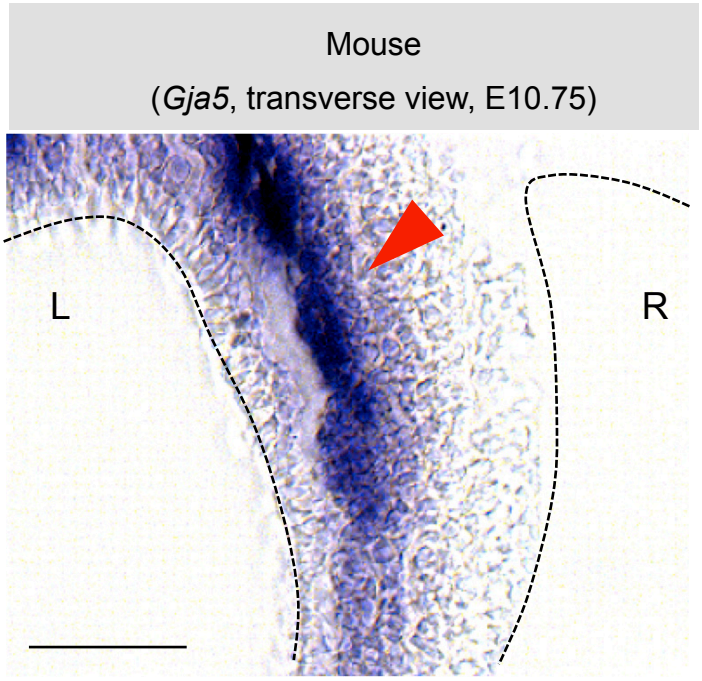

Fig. S4

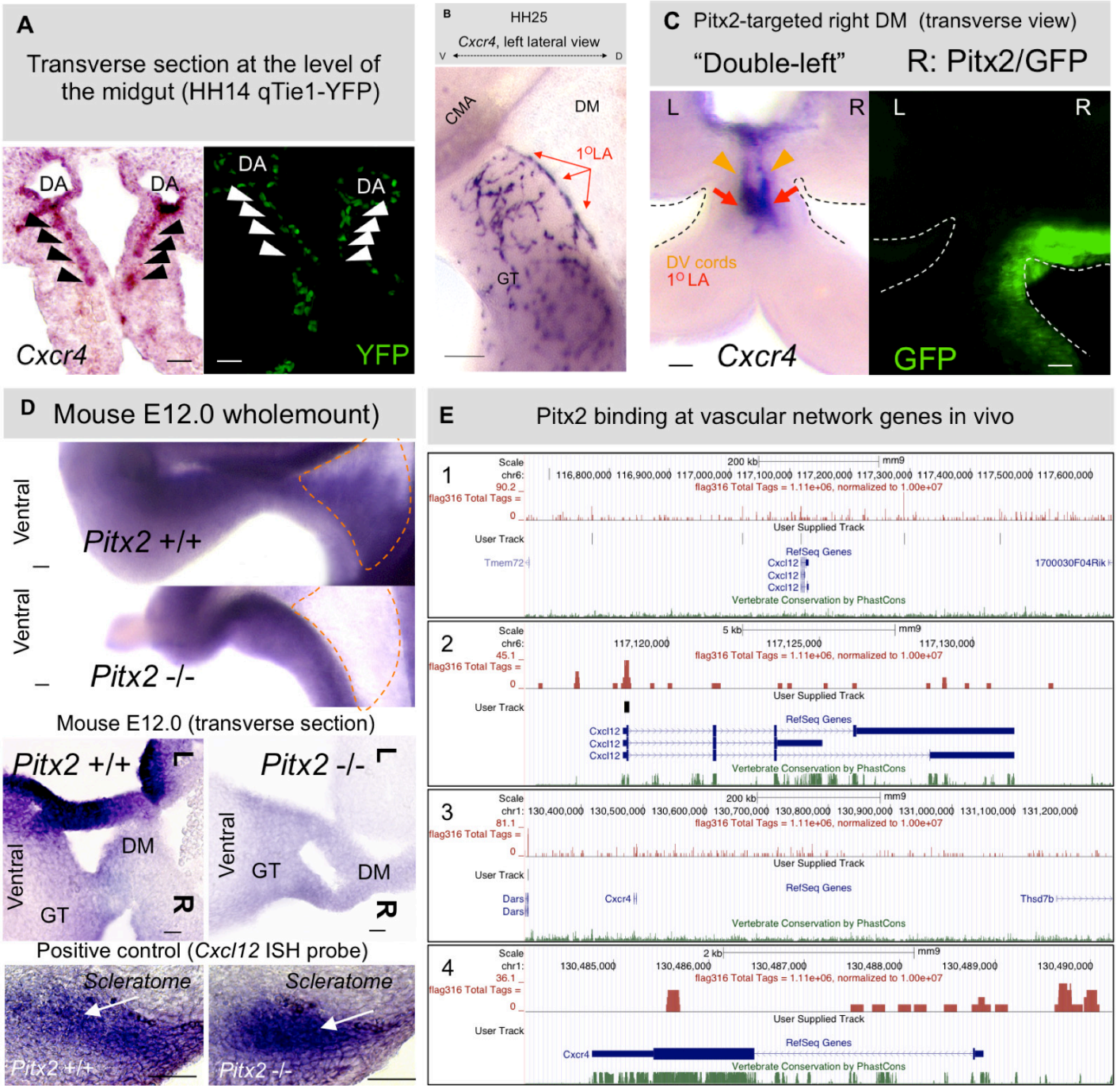
A
Transverse section at the level of the midgut (HH14 qTie1-YFP)
DA
DA
DA
DA
Cxcr4
YFP
B
HH25
Cxcr4, left lateral view
V
D
CMA
DM
1°LA
GT
C
Pitx2-targeted right DM (transverse view)
"Double-left"
R: Pitx2/GFP
L
R
L
R
DV cords
1°LA
Cxcr4
GFP
D
Mouse E12.0 wholemount)
Ventral
Pitx2 +/+
Ventral
Pitx2 -/-
Mouse E12.0 (transverse section)
Pitx2 +/+
Pitx2 -/-
Ventral
DM
GT
R
Ventral
GT
DM
R
Positive control (Cxcl12 ISH probe)
Scleratome
Scleratome
Pitx2 +/+
Pitx2 -/-
E
Pitx2 binding at vascular network genes in vivo
1
Scale
chr6:
200 kb
mm9
116,800,000 116,900,000 117,000,000 117,100,000 117,200,000 117,300,000 117,400,000 117,500,000 117,600,000
90.2
flag316 Total Tags =
flag316 Total Tags = 1.11e+06, normalized to 1.00e+07
0
User Supplied Track
User Track
RefSeq Genes
Tmem72
Cxcl12
Cxcl12
Cxcl12
1700030F04Rik
Vertebrate Conservation by PhastCons
2
Scale
chr6:
5 kb
mm9
117,120,000
117,125,000
117,130,000
45.1
flag316 Total Tags =
flag316 Total Tags = 1.11e+06, normalized to 1.00e+07
0
User Supplied Track
User Track
RefSeq Genes
Cxcl12
Cxcl12
Cxcl12
Vertebrate Conservation by PhastCons
3
Scale
chr1:
200 kb
mm9
130,400,000 130,500,000 130,600,000 130,700,000 130,800,000 130,900,000 131,000,000 131,100,000 131,200,000
81.1
flag316 Total Tags =
flag316 Total Tags = 1.11e+06, normalized to 1.00e+07
0
User Supplied Track
User Track
RefSeq Genes
Dars
Dars
Cxcr4
Thsd7b
Vertebrate Conservation by PhastCons
4
Scale
chr1:
2 kb
mm9
130,485,000
130,486,000
130,487,000
130,488,000
130,489,000
130,490,000
36.1
flag316 Total Tags =
flag316 Total Tags = 1.11e+06, normalized to 1.00e+07
0
User Supplied Track
User Track
RefSeq Genes
Cxcr4
Vertebrate Conservation by PhastCons

Fig. S5

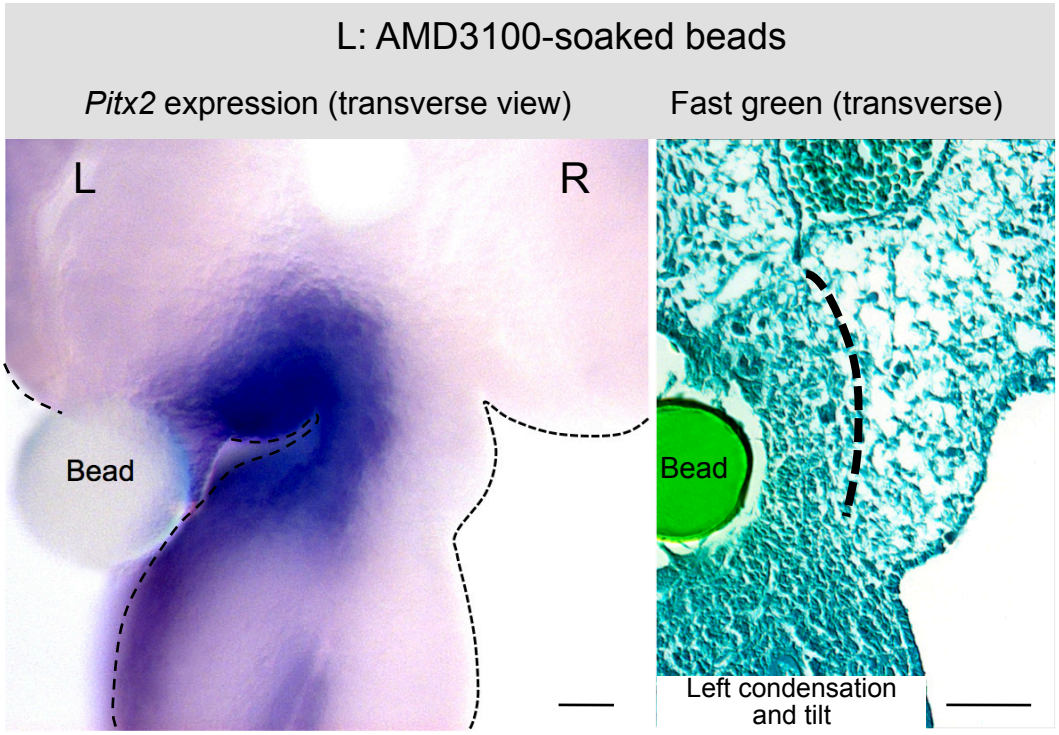
L: AMD3100-soaked beads
Pitx2 expression (transverse view)
Fast green (transverse)
L
R
Bead
Bead
Left condensation and tilt

Fig. S6

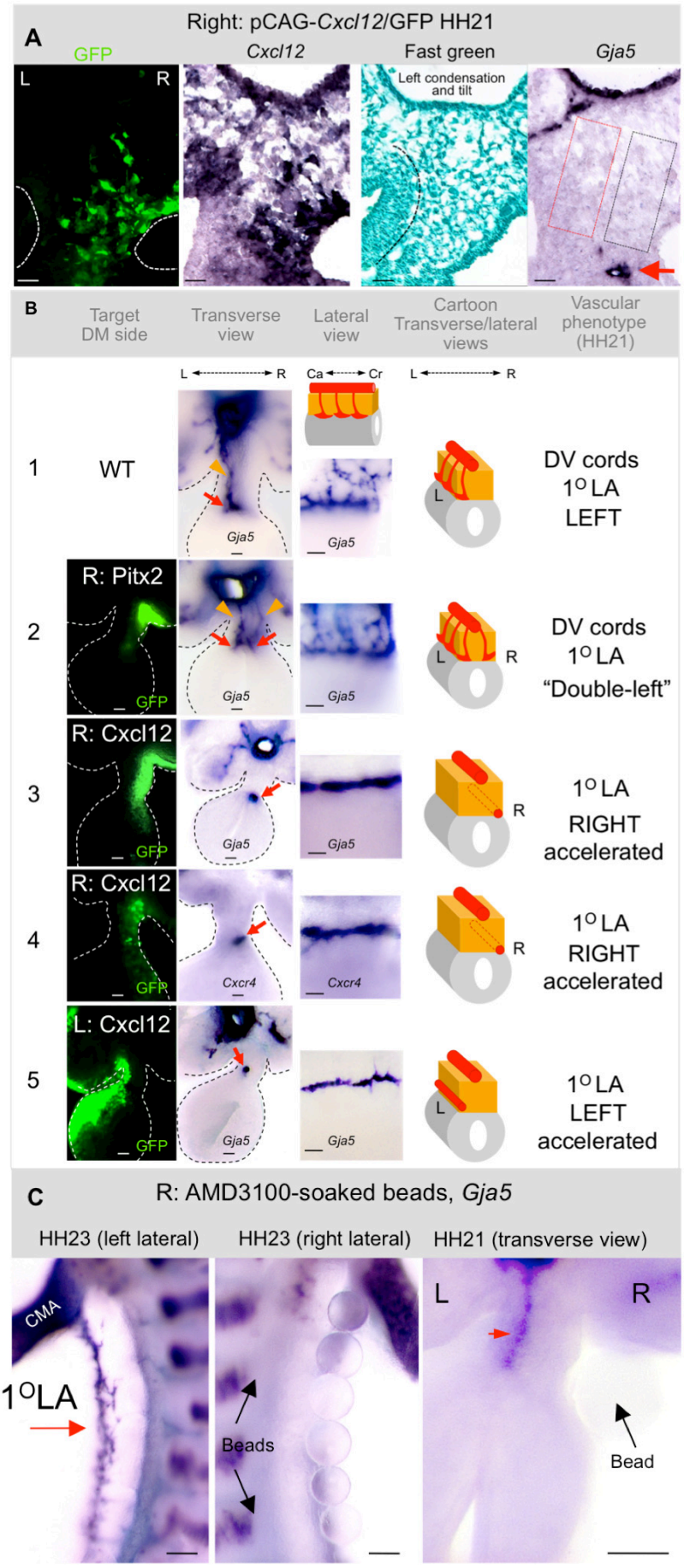
A
Right: pCAG-Cxcl12/GFP HH21
GFP
Cxcl12
Fast green
Gja5
L
R
Left condensation and tilt
B
Target DM side
Transverse view
Lateral view
Cartoon Transverse/lateral views
Vascular phenotype (HH21)
1
WT
DV cords 1O LA LEFT
2
R: Pitx2
DV cords 1O LA "Double-left"
3
R: Cxcl12
1O LA RIGHT accelerated
4
R: Cxcl12
Cxcr4
1O LA RIGHT accelerated
5
L: Cxcl12
1O LA LEFT accelerated
C
R: AMD3100-soaked beads, Gja5
HH23 (left lateral)
HH23 (right lateral)
HH21 (transverse view)
CMA
1OLA
Beads
Bead

Fig. S7

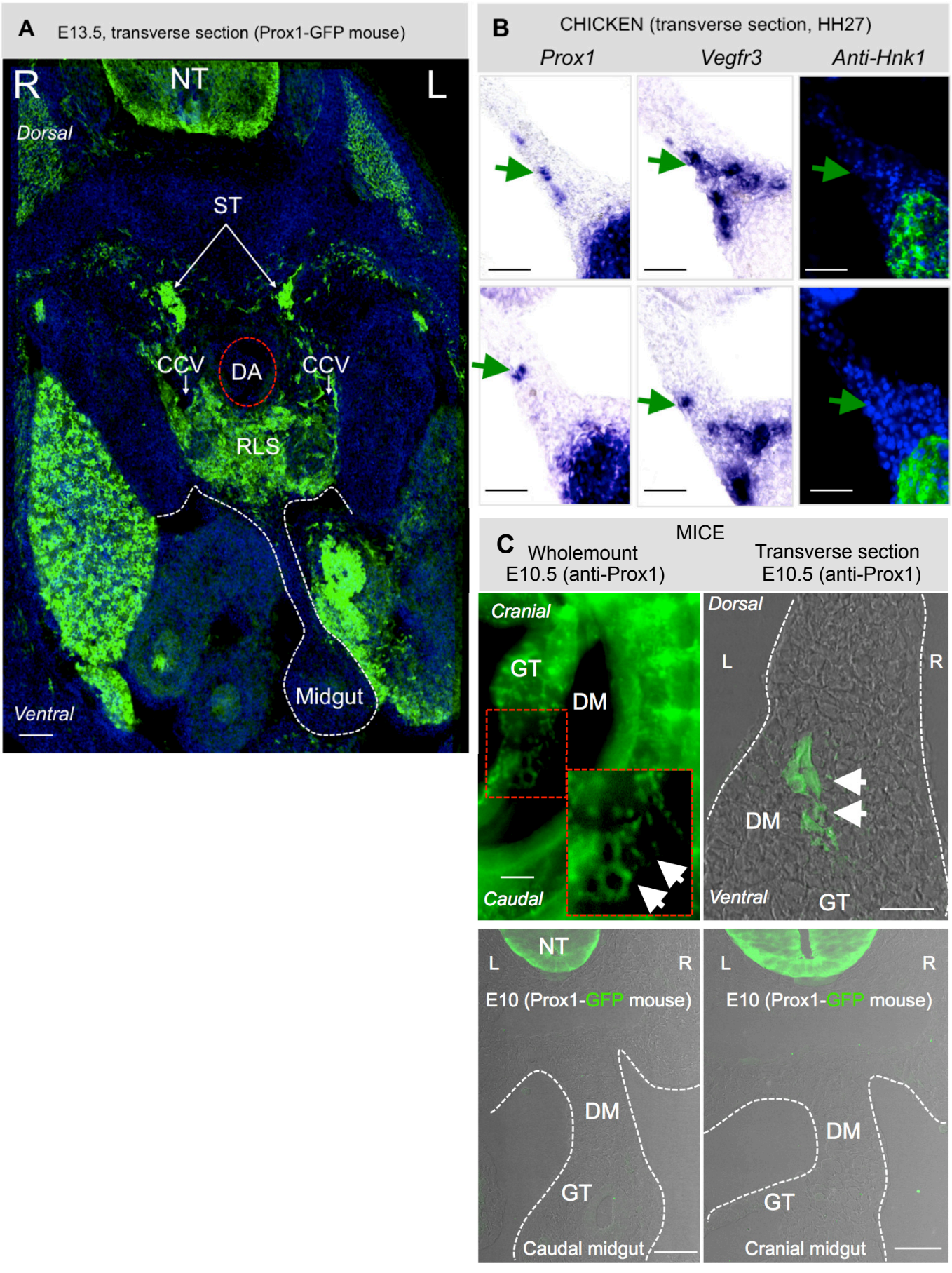
A
E13.5, transverse section (Prox1-GFP mouse)
R
NT
L
Dorsal
ST
CCV
DA
CCV
RLS
Midgut
Ventral
B
CHICKEN (transverse section, HH27)
Prox1
Vegfr3
Anti-Hnk1
C
MICE
Wholemount
E10.5 (anti-Prox1)
Transverse section
E10.5 (anti-Prox1)
Cranial
GT
DM
Caudal
Dorsal
L
R
DM
Ventral
GT
NT
L
R
E10 (Prox1-GFP mouse)
DM
GT
Caudal midgut
L
R
E10 (Prox1-GFP mouse)
DM
GT
Cranial midgut

Fig. S8

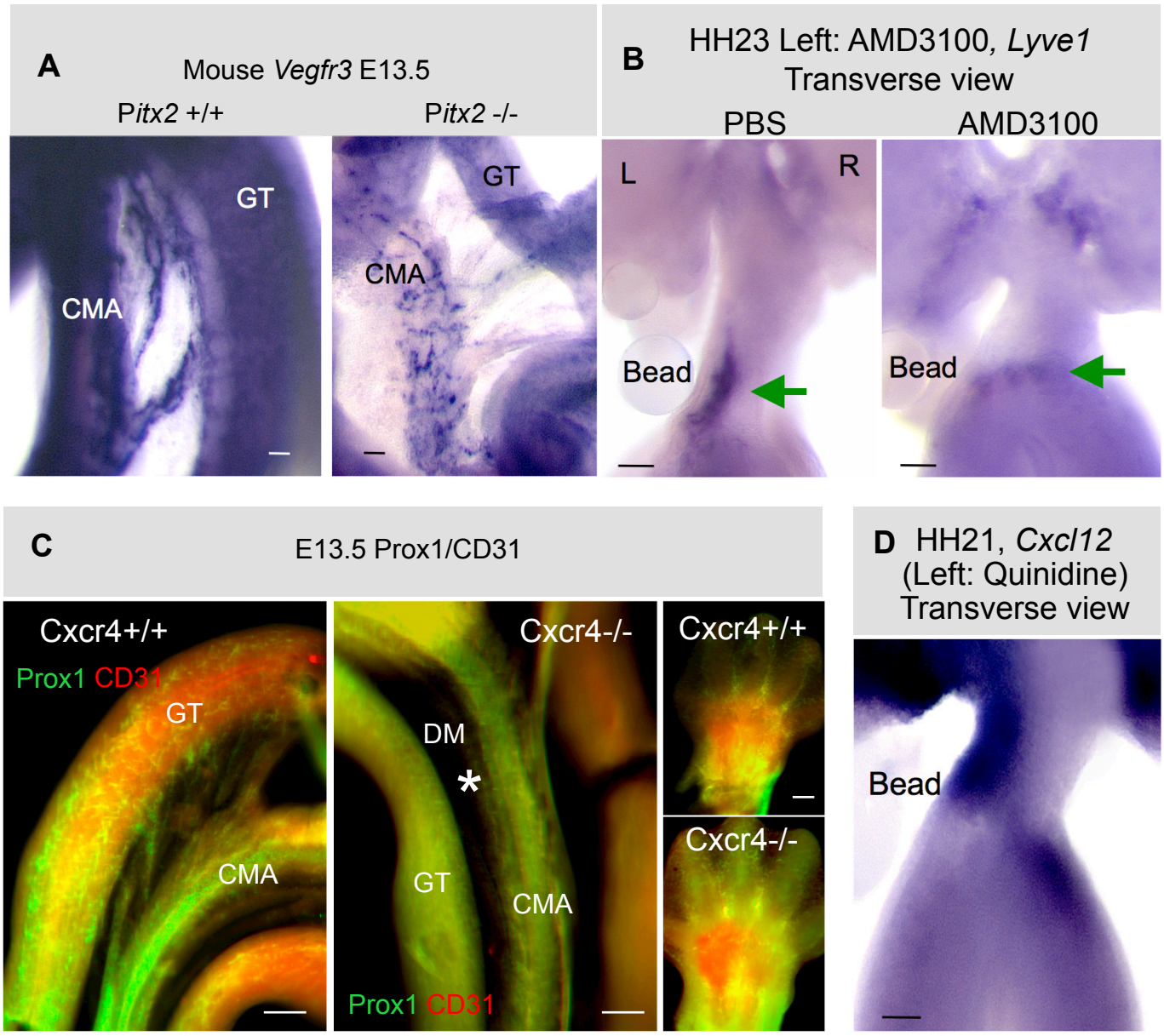
A
Mouse Vegfr3 E13.5
Pitx2 +/+
Pitx2 -/-
GT
CMA
GT
CMA
B
HH23 Left: AMD3100, Lyve1
Transverse view
PBS
AMD3100
L
R
Bead
Bead
C
E13.5 Prox1/CD31
Cxcr4+/+
Prox1 CD31
GT
CMA
Cxcr4-/-
DM
*
GT
CMA
Prox1 CD31
Cxcr4+/+
Cxcr4-/-
D
HH21, Cxcl12
(Left: Quinidine)
Transverse view
Bead

Supplemental Figure Legends

Fig. S1. Validation of laser capture microdissection transcriptional analyses of the chicken DM (related to Fig. 1). In situ hybridization at HH21, using indicated probes. Scale bars: 50 μm.

Fig. S2. Live imaging setup for time lapse of transient D-V cords and TUNEL assay (related to Fig. 2). A Tie-1 H2B-YFP transgenic quails with wholemount view (**B**) of D-V endothelial cords. **C** Embryos are sliced into 150 μm transverse sections and then (**D**) embedded in low melting point agarose for imaging on glass-bottom culture plates. **E** Example of YFP fluorescent tissue slice, showing bilateral (left panel) and left-sided (right panel) endothelial cords; these panels are simplified in a cartoon model (**G**). (**H-J**) TUNEL assay of Tie-1 H2B-YFP transgenic quails demonstrating in **H** the absence of TUNEL-positive cells (red) in the DM and in Tie-1 H2B-YFP expressing endothelial cells (green, arrowhead); TUNEL-positive cells in the apoptotic mesonephros (MSN, boxed region of **H** is magnified in **I**) and in the limb bud AER (apical ectodermal ridge, **J**, from the same embryo as **H**). Scale bars: **A** 500 μm; **B,C** 200 μm; **D** 1.5 cm; **E,F,H** 50 μm; **I** 10 μm; **J** 20μm.

Fig. S3. Analysis of arterial vasculogenesis in chicken and mice (related to Fig. 3). Asymmetric formation of D-V cords in mice at E.10.75 (*Gja5*). Scale bar: 50 μm.

Fig. S4. Analysis of Cxcr4/Cxcl12 expression downstream of Pitx2 (related to Fig. 4). A ISH at HH14 (chicken) reveals *Cxcr4* expression (**left panel**) in Tie1-expressing (H2B-YFP, **right panel**) endothelial cells of the bilateral intervening plexus (black arrowheads). **B** Later, Cxcr4

expression is found both in the 1^0LA and gut plexus, but not the CMA. **C**, Misexpression of Pitx2/GFP in the right DM (right panel GFP marks electroporated cells) causes left isomerism ("double-left" phenotype) including double *Cxcr4*-positive arterial cords (orange arrowheads) and duplicated 1^0LA (red arrows). **D** Loss of *Cxcl12* expression in the DM of *Pitx2*-/- mouse (E12.0), with left lateral (**top two rows**) and transverse views shown (**third row**). Positive control tissue from matched embryos (**bottom row**) reveals Cxcl12 staining in the scleratome. **E** Pitx2 binding at vascular network genes in vivo. (**1-2**) 5 enriched Pitx2 binding peaks surround *Cxcl12* (**1**), one of which directly overlaps with exon 1 on *Cxcl12* (**2**). (**3-4**) No significant Pitx2 binding is observed at the *Cxcr4* locus, the promoter of the adjacent gene *Dars* contains an enriched peak (**3**) but no peaks are observed in the promoter proximal region of *Cxcr4* (**4**). ChIP-seq data derive from published transgenic FLAG-tagged Pitx2 binding in 12-week mouse cardiac tissue (NCBI Gene Expression Omnibus (GEO) data repository accession GSE50401): top green track shows normalized ChIP-seq tag numbers (y-axis) and the user supplied track below shows peaks with at least 4-fold enrichment over input control indicated as vertical black bars. RefSeq gene models are indicated in blue, while bottom track shows PhastCons vertebrate conservation score in green. Scale bars: **A** 20 μm; **B** 200 μm; **C,D** 50 μm.

Fig. S5. Side-specific effects of AMD3100 inhibitor-soaked beads on *Pitx2* expression and DM morphology (related to Fig. 5). AMD3100 has no effect on normal left-sided *Pitx2* expression (**left panel**) or cellular morphology (**right panel**) of the DM. Scale bars: 50 μm.

Fig. S6. Cxcl12 is not sufficient to drive vessel formation in the absence of *Pitx2* (related to Fig. 6). **A** Misexpression of Cxcl12 (pCAG-Cxcl12/pCAG-GFP) on the right side via co-

electroporation produces normal L-R DM cellular morphology (fast green), results in ectopic levels of Cxcl12 that exceed those on the left side (ISH, *Cxcl12*), and is not sufficient to promote formation of ectopic D-V cords in the right DM (ISH, *Gja5*, black dashed box). **B** Results of left-sided and right-sided targeting of Cxcl12 in the DM at HH21 (ISH, *Gja5*, model cartoon included). Transverse views shown to appreciate L-R situs and lateral view (Cranial-Caudal) to appreciate the extent of 1^0LA formation. (**1**) Wild type DM showing left-sided D-V cord (orange arrowhead) and 1^0LA formation (red arrow). (**2**) 'Double-left' phenotype with right-sided Pitx2 electroporation (GFP) showing left- and right-sided D-V cords and two 1^0LA. (**3**) Right-sided Cxcl12 electroporation (GFP) showing ectopic 1^0LA forming on the right side as a result of accelerated remodeling of the left-sided, Cxcr4-positive (**4**) D-V cords (see also Fig. 6). This result is in contrast to (**2**) highlighting an important functional difference between Pitx2 and Cxcl12 in the DM. (**5**) Left-sided Cxcl12 electroporation (GFP) showing accelerated formation of 1^0LA as a result of accelerated remodeling of the left-sided D-V cords. **C** The diffusion range of AMD3100 inhibitor does not allow it to cross the midline boundary of the DM: inhibitor beads placed on the right side (**middle panel**, right lateral view) have no effect on the normal left-sided assembly of endothelial cords (**right panel,** arrowhead) and 1^0LA (**left panel**, arrow). Bead positions are indicated. Scale bars: **A-B** 50 μm; **C** 100 μm.

Fig. S7 Lymphatic marker expression in tissues surrounding the DM (related to Fig. 7). A Prox1-GFP-marked lymphatic anlagen in the retroperitoneal lymph sac (RLS), caudal cardinal veins (CCV) and non-lymphatic staining in the sympathetic trunk (ST) and neural tube (NT). **B** Adjacent transverse sections showing that location of lymphatic anlagen (green arrows) in three different HH27 chicken embryos, marked by *Prox1* (**left column**) and *Vegfr3* (**middle column**)

is spatially distinct from *Prox1*-expressing cells of the avian-specific Nerve of Remak (Hnk1-positive, **right column**). **C Top row** Wholemount (left) and transverse views (right) of wild type mouse DM stained with anti-Prox1; lymphatic plexus is first visible ventrally (white arrows, higher magnification inset) that extends dorsally. **Bottom row** Absence of Prox1-GFP reporter signal in mouse cranial or caudal DM prior to E10.5, revealed by transverse section of E10 Prox1 transgenic reporter mice. Scale bars: **A 100** μm; **B** 50 μm; **C** (top left panel) 100 μm (top right panel) 20 μm (bottom panels) 50 μm.

Fig. S8 Local lymphangiogenesis in the left DM requires the preceding Pitx2-driven arterial program (related to Fig. 8). A *Vegfr3* expression (ISH) is absent from *Pitx2*-/- mutant DM at E13.5 but remains unchanged along the CMA. **B**, Cxcr4/Cxcl12-inhibiting AMD3100 beads (**right panel**) on the left side of the chicken DM abrogate the *Lyve1*-positive network (HH23), compared to PBS beads (**left panel**). **C** Wholemount double immunohistochemistry for Prox1 (green) and PECAM/CD31 (red) reveals loss of Prox1 staining (asterisk) in the DM of Cxcr4 -/- mutant mouse embryos at E13.5 (**middle panel**) compared to wild type littermates (**left panel**). Peripheral limb lymphatics are unchanged in matched embryos (**right column**). **D** Arteriogenesis-inhibiting Quinidine beads on the left side of the chicken DM have no effect on *Cxcl12* expression (HH21). Scale bars: **A**,**B,D** 50 μm; **C** 100 μm.

Movie S1. **Right-sided endothelial cord regression in midgut explants of Tie-1-H2B-eYFP quail embryos (related to Fig. 2 and Fig. S2). Left panel:** Select nuclei of endothelial cells of right DM were manually tracked with dragon tails (Bitplane Imaris software). **Right panel**: Tracking of select endothelial nuclei of the left cord (green), right cord (red) and dorsal aorta

(blue). At time T=0 (HH17, 60 hours), bilateral endothelial cords are present in the DM. At T=4.5 hours (HH18, 65 hours), cells of the right side endothelial cords have significantly regressed and by T=6.5 hours (HH19, 70.5 hours) the regression is complete.

Movie S2. Right to left endothelial cell migration in midgut explants of Tie-1-H2B-eYFP quail embryos (related to Fig. 2 and Fig. S2). Left panel: Select nuclei of endothelial cells of right DM were manually tracked with dragon tails (Bitplane Imaris software). **Right panel**: Tracking of select endothelial nuclei of the left cord (green), right cord (red) and dorsal aorta (blue). Starting at HH19, time-lapse imaging reveals that cells within right-sided endothelial cords regress, migrate and anastomose with the left endothelial cords giving rise to vasculature asymmetries in the DM.

Movie S3: Complete regression and endothelial cell emigration of right-sided arterial cord (related to Fig. 2 and Fig. S2). Left panel: Time-lapse of Tie-1 H2B-eYFP quail embryo midgut explants shows remodeling of the intervening endothelial plexus to yield the left DV arterial cord. At time T =0 (HH17), bilateral endothelial cords are present in the DM. At T=5 hours (HH18), cells of the right side endothelial cords have significantly regressed and by T=10.5 hours (HH19) regression is complete. By T =13.5 hours (HH20) we find that regressed cells from the right migrate left and contribute to the left endothelial cord. **Right panel:** Select nuclei of endothelial cells of the left and right cord, and left and right dorsal aortae are labeled with green, red, purple and blue spots, respectively; tracking of these spots models the cell movements in the left panel movie.